Accepted Manuscript

Synthesis and *in vitro* evaluation of novel triazine analogues as anticancer agents and their interaction studies with bovine serum albumin

Prinka Singla, Vijay Luxami, Kamaldeep Paul

PII: S0223-5234(16)30271-9

DOI: 10.1016/j.ejmech.2016.03.088

Reference: EJMECH 8513

To appear in: *European Journal of Medicinal Chemistry*

Received Date: 31 January 2016

Revised Date: 30 March 2016

Accepted Date: 31 March 2016

Please cite this article as: P. Singla, V. Luxami, K. Paul, Synthesis and *in vitro* evaluation of novel triazine analogues as anticancer agents and their interaction studies with bovine serum albumin, *European Journal of Medicinal Chemistry* (2016), doi: 10.1016/j.ejmech.2016.03.088.

Graphical Abstract

Synthesis and *in vitro* evaluation of novel triazine analogues as anticancer agents and their interaction studies with bovine serum albumin

Prinka Singla, Vijay Luxami* and Kamaldeep Paul*

School of Chemistry and Biochemistry, Thapar University, Patiala-147 004, INDIA

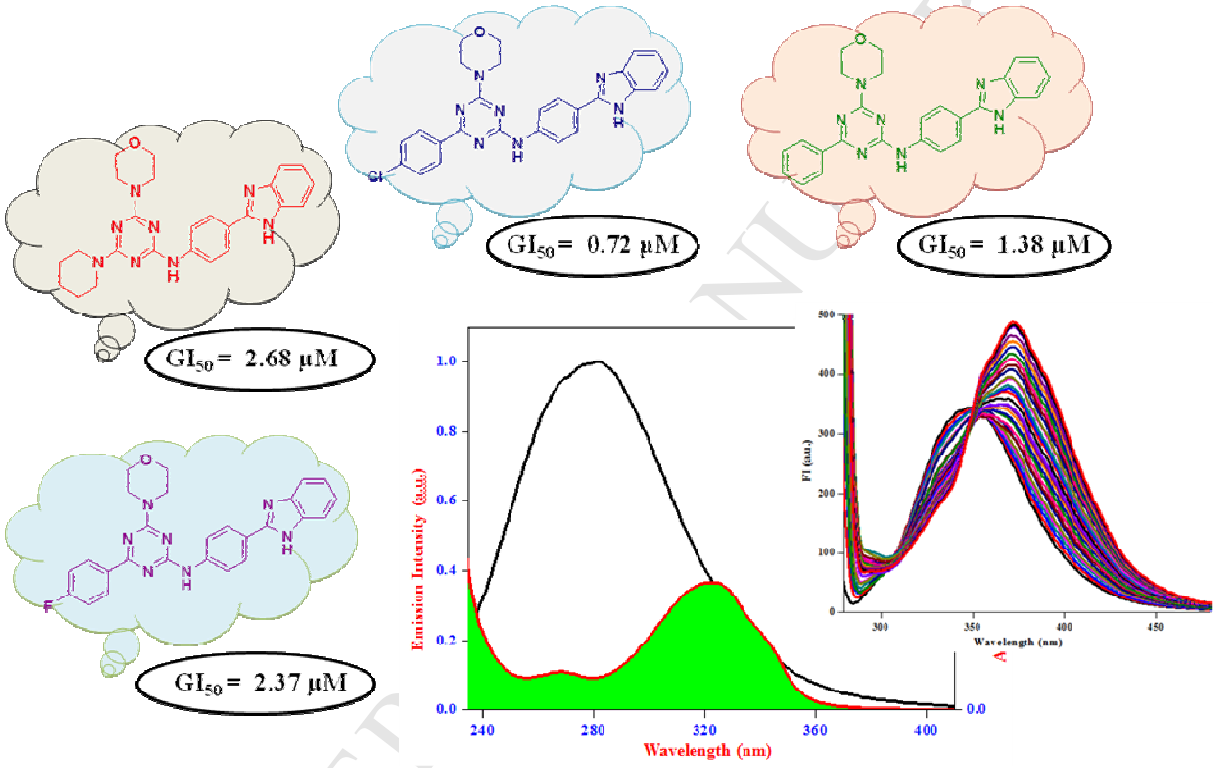

Synthesis and *in vitro* evaluation of novel triazine analogues as anticancer agents and their interaction studies with bovine serum albumin

Prinka Singla, Vijay Luxami* and Kamaldeep Paul*

School of Chemistry and Biochemistry, Thapar University, Patiala-147 004, India

*E-mail: kpaul@thapar.edu (K. Paul), vluxami@thapar.edu (V. Luxami)

Abstract

A novel series of triazine-benzimidazole analogs has been designed and synthesized for their *in vitro* anticancer activities. Four compounds (**6**, **16**, **17** and **20)** were identified as highly potent anticancer agents against 60 human cancer cell lines with GI_{50} in the nanomolar range. To improve the drug applications toward cancer cells, there is a need to couple these compounds to some carrier macromolecules. Following this approach, the interaction between triazine-benzimidazole analogues and bovine serum albumin (BSA) has been investigated with UV-Visible and fluorescence spectroscopic methods under physiological conditions. The observed fluorescence quenching indicates that these compounds could efficiently bind with BSA and be transported to the target site.

Keywords: Triazine, Benzimidazole, Antitumor activity, Bovine serum albumin, Fluorescence resonance energy transfer.

1. Introduction

Cancer is considered one of the world's most devastating disease [1]. Millions of new cases are reported every year with high mortality. Improvements in treatment and prevention led to diminish the cancer deaths. Considerable efforts are given to identify molecules with anticancer properties from both natural and synthetic sources [2]. It is well-known that heterocyclic compounds are abundant and their structural subunits exist in many natural products such as vitamins, hormones, antibiotics, alkaloids and pharmaceuticals. Among the wide variety of synthetic compounds recognized as potential anticancer drugs, molecules based on triazine [3] and benzimidazole [4] scaffolds have attracted great interest. Several reports describing evaluation of triazine derivatives as antitumor agents appeared in the recent literature [5-7]. For example, HL010183 [8] and irsogladine [9], possess antiangiogenic and anticancer properties. Similarly, lysophosphatidic acid acyltransferase-β inhibitor (CT32228), demonstrates a very good antileukemic profile [10]. The triazine ring in

altretamine (hexamethylmelamine) is typically responsible for anticancer activity [11]. Gedatolisib with triazine ring has been found to be the dual phosphoinositide 3-kinase and mTOR kinase inhibitors, which is currently under clinical trials [12]. This structural motif is also present in reversing anticancer multidrug transport inhibitor of ABCG2 transporter (PZ-39) [13] and in an aromatase inhibitor (SEF19) (Figure 1) [14]. Herein, our strategy is to discover new cancer chemotherapeutic agents using a small molecule library that contained triazine and benzimidazole core structures.

Figure 1

It has been observed that low antiproliferative activity of heterocyclic compounds is due to restricted access to the target site. This limitation has hindered the potential clinical use of heterocyclic compounds. A promising approach to improve their efficacy towards cancer cells is to couple anticancer drugs to carrier macromolecules. Various types of macromolecules have been used including poly(ethyleneglycol) polymer, nanoparticles, nanotubes, liposomes, dendrimers and protein biomolecules [15]. Among these, bovine serum albumin (BSA) is used as a promising drug delivery system owing to abundance in plasma. Serum albumin transporter acts as carriers of endogenous and exogenous compounds [16] including fatty acids, amino acids, drugs, and pharmaceuticals for improvement of pharmacokinetic and pharmacodynamic behavior of several drugs. In addition, owing to its biochemical and pharmacological properties, BSA has also been used to target diseased and malignant cells as a versatile drug carrier; resulting in higher efficacy of treatment and reduced side effects [17-19]. The binding pocket of BSA, with two tryptophan residues (Trp-134 and Trp-212) and phenylalanine possesses intrinsic fluorescence [20] and binding changes the fluorescent signal, providing a convenient method to understand structural changes. Therefore, in the present study we have studied the interactions of triazine-benzimidazoles and BSA by using UV-Visible and fluorescence spectroscopic techniques. This method further allowed the determination of binding parameters such as binding constant, number of binding sites, and binding distance of compounds and BSA, which helped in elucidate the binding probability.

2. Results and Discussion

2.1. Chemistry

Triazine-benzimidazoles **(5-21)** were prepared as shown in **scheme 1**. Cyanuric chloride was stirred with morpholine in the presence of sodium bicarbonate in THF at 0-5 ^{o}C for 6 h to give 4,6-dichloro-2-morpholin-4-yl-[1,3,5]triazine (**2**) in 89% yield. Condensation of 4-

aminobenzoic acid with *o*-phenylenediamine in the presence of polyphosphoric acid at 200 ^{o}C for 5 h afforded 4-(1*H*-benzimidazol-2-yl)-phenylamine (**3**) as white solid. Compound **2** was underwent nucleophilic substitution reaction with 4-(1*H*-benzimidazol-2-yl)-phenylamine (**3**) in the presence of potassium carbonate and THF at room temperature for 24 h, furnished [4-(3*H*-benzimidazol-5-yl)-phenyl]-(6-chloro-2-morpholin-4-yl-[1,3,5]triazin-2-yl)-amine (**4**) in 84 % yield. Further, treatment of compound **4** with different primary and secondary amines in the presence of potassium carbonate and 1,4-dioxane at 110 ^{o}C for 8-12 h gave compounds **5-15** in 64-78% yields. Various five and six member aryl groups like furan, thienyl and phenyl were also substituted with compound **4** via Suzuki-Miyuara cross coupling reaction in the presence of 10 mol% of $Pd(PPh_3)_4$ and 1.5 equivalents of K_2CO_3 in 1,4-dioxane to afford compounds **16-21** in good yields (65-72%). The structures of newly synthesized compounds were confirmed by ^{1}H and ^{13}C NMR as well as mass spectrometry (Supporting Information).

Scheme 1

2.2. In Vitro anticancer screening

Compounds **5-21** were submitted to the National Cancer Institute (NCI), Bethesda, Maryland, USA for evaluation of antitumor activities. Four compounds (**6, 16, 17** and **20**) were selected for *in vitro* studies against 60 human cancer cell lines at one dose concentration of 10 μM. Structures are generally selected for screening based upon drug-like properties utilizing the concept of privileged scaffolds or structures based on computer-aided design. *In vitro* antitumor screening data revealed that triazine with piperidine (**6**), phenyl (**16**), 4-fluorophenyl (**17**) and 4-chlorophenyl (**20**) substitutions showed significant inhibitory activity towards most of the cancer cell lines. Compounds **6**, **16**, **17** and **20** were found to be broad spectrum against all nine subpanels of cancer cell lines at primary single dose concentration (10 μM) with mean growth percent of 0.72, -56.41, -7.32 and -83.19 respectively. Close examination of the data presented in Table 1 indicated that compounds **16** and **20** have been found to be most potent while **6** and **17** showed moderate antitumor activities.

Table 1

These four compounds were further screened against cell lines representative of the 9 different cancer types, at five doses (0.01-100 μM) to determine GI_{50}, TGI and LC_{50}. Results indicated these compounds were very effective against two leukemia cancer cell lines: HL-60 (TB) and SR, with GI_{50} values in the nanomolar range. HL-60 (TB) appeared to be the most sensitive to compound **16**, exhibiting a GI_{50} value of 31 nM with TGI value of 601 nM.

Similarly, compounds **6**, **16**, **17** and **20** also showed effective growth inhibition against leukemia cancer cell line SR with GI_{50} values of 731 nM, 125 nM, 539 nM and 31 nM, respectively. All four compounds were also active against renal cancer cell line RXF393 with respective GI_{50} values of 808 nM, 501 nM, 459 nM and 222 nM. Compound **20** (MG MID GI_{50} value of 720 nM) is almost four fold, two fold and three fold more active than compounds **6**, **16** and **17** with MG MID GI_{50} values of 2680 nM, 1380 nM and 2370 nM respectively (Table 2 and Figures S39-S54) [21-24].

Table 2

2.3. Bovine serum albumin interactions.

To examine the structural interaction of bovine serum albumin (BSA) with compounds **5-21**, absorbance and emission spectral measurements were carried out. The UV-visible spectrum of BSA (10 μM) showed an intense band at 279 nm in phosphate buffer at pH 7.4 that arises due to the presence of phenyl rings in Trp (tryptophan), Tyr (tyrosine), and Phe (phenylalanine) residues. Subsequent addition of compounds **5-14**, **16**, **17** and **20** to BSA solution resulted in a gradual increase in the intensity of peak at 279 nm with the appearance of new band at 324 nm. These changes in absorbance clearly indicated the interaction of compounds with BSA and leading to an increase of hydrophobicity in the vicinity of Trp, Tyr and Phe residues (Figure 2). As shown in Table 3, the addition of compounds **5-14, 16, 17** and **20** to BSA resulting in hyperchromicity within range of 65.29% - 97.67% (Figures S55-S63), while compounds **15, 18, 19** and **21** did not show any significant change with BSA. Moreover, the maximum absorption wavelength of BSA remains unchanged, implying that the interactions between compounds and BSA are non-covalent in nature and likely occur through $\pi-\pi$ stacking between aromatic rings of compounds and phenyl rings of Trp, Tyr and Phe residues located in the binding cavity of BSA.

Figure 2

These interaction studies were further investigated through fluorescence spectroscopy. On excitation at 280 nm, the emission spectrum showed an intense band at 350 nm. The emission is sensitive to changes in local environment of the Trp-134 and Trp-212 and so can be attenuated by binding of a small molecule at or near this residue. In all cases, 350 nm fluorescence emission of the protein was decreased with increasing concentrations of compounds **5-14**, **16**, **17** and **20**, indicating the binding of compounds to the protein. The decrease in the fluorescence intensity of BSA at 350 nm was accompanied by the

enhancement of new band within the range of 370 nm and 373 nm, which is attributed to formation of a complex between compounds and protein (Figure 3 and Figures S55-S63).

Figure 3

These absorption and emission results indicated that the microenvironment of the three aromatic acid residues might be altered and the tertiary structure of BSA destroyed. Compounds **15**, **18**, **19** and **21** did not show any significant change with the conformation of BSA, indicating for the requirement of linker or heteroatom at C-6 position of triazine. As a result all further testing was carried out on compounds **5-14**, **16**, **17** and **20**. The changes in absorption and fluorescence intensities clearly indicated the interacting properties of triazine-benzimidazoles with BSA. When a small molecule binds independently to a set of equivalent sites on a macromolecule, the photophysical properties, binding constants (determined by Benesi–Hildebrand equation) [25] and the numbers of binding sites (n) (using double-logarithmic equation) [26,27] can be determined. In this way, we quantitated the binding strength between triazine-benzimidazole analogues and BSA. The binding constant of complexes confirmed a significant role for the configuration of triazine-benzimidazole analogues around BSA as shown in Table 3. The linear fitting plots of respective $1/(A_0\text{-}A)$ and $1/(F_0\text{-}F)$ vs. 1/[compounds] (Inset Figures 2 and 3) were observed for the interaction between BSA and compounds **5-14**, **16**, **17** and **20** (Figures S55-S63). The value of n is helpful to know the number of binding sites for compounds and BSA which in most of the cases has been found to be nearly 1. Thus, there was one independent class of binding site on BSA for compounds, and the molar ratio of protein to compounds **5-14**, **16**, **17** and **20** is 1:1 in the binding reactions.

Table 3

2.4. Energy transfer between triazine-benzimidazole analogues and BSA

To further confirm the vicinity of the analogues to the BSA (distance between compound and BSA) [28,29], fluorescence resonance energy transfer (FRET) from protein to ligands was verified. According to the Förster theory of non-radioactive energy transfer, the transfer of energy can take place through a direct electrodynamic interaction between the primarily excited molecule and its neighbour. Using the fluorescence resonance energy transfer (FRET), the distance r of binding between compounds **5-14**, **16**, **17** and **20** and BSA has been calculated by the equation-1 [30].

$$E = 1 - \frac{F}{F_0} = \frac{R_0^6}{R_0^6 + r^6} \quad \text{--------1}$$

where E denotes the efficiency of energy transfer between donor and acceptor, r is the distance between donor and acceptor, and F and F_0 are fluorescence intensities of BSA in the presence and absence of quencher, respectively. R_0, the critical energy transfer distance when the transfer efficiency is 50%, is given by the equation-2 [31].

$$R_0 = 8.79x10^{-25}\left[K^2 n^{-4} \Phi J\right] \quad \text{---------2}$$

K^2 is the orientation factor of the donor and acceptor dipoles, *n* is the refraction index of medium, Φ is the fluorescence quantum yield of the donor in the presence of acceptor, and *J* expresses the degree of spectral overlap between the donor emission and the acceptor absorption, which could be calculated by the equation-3:

$$J = \frac{\int_0^\infty F(\lambda)\varepsilon(\lambda)\lambda^4 d\lambda}{\int_0^\infty F(\lambda) d\lambda} \quad \text{-----3}$$

where F(λ) is the normalized donor emission spectrum in the range from λ to λ + Δλ, and ε(λ) is the molar absorption coefficient of the acceptor at wavelength λ. According to the above equations (eq. 1-3) and using K^2 = 2/3, n = 1.33 and Φ = 0.15 [32], *J*, R_0, r, and E were calculated (Table 4). On gradual addition of compounds **5-14**, **16**, **17** and **20**, fluorescence intensity of the tryptophan residue (Trp-212) present in BSA decreased with a concomitant increase in the fluorescence intensity through an isoemissive point within range of 339 nm and 357 nm (Figure 3, Table 3). This indicates an efficient energy transfer from the tryptophan residue (Trp-212) present in BSA to compounds **5-14**, **16**, **17** and **20** (Figures S64-S67). The overlap of absorption spectrum of compounds **6**, **16**, **17** and **20** and the emission spectrum of BSA are shown in Figure 4. It has been observed that distance (r) between the Trp residue (as donor) and the interacting compound (as acceptor) is in the range of 4−8 nm. According to Valuer *et. al*., the maximum academic value for R_o should be < 10 nm and r should be less than 8 nm [33]. In the present study, both R_o and r values are well within the permissible limits. These results indicated that the energy transfer from BSA to compounds occur with high probability.

Figure 4

Table 4

3. Conclusions

In summary, a series of novel substituted triazine-benzimidazole analogs have been synthesized and characterized by ^{1}H and ^{13}C NMR. These compounds were evaluated for growth inhibition properties against a panel of 60 human cancer cell lines, and their GI_{50}, TGI and LC_{50} values have been determined. Four compounds (**6**, **16**, **17** and **20**) have been identified with GI_{50}'s in the nanomolar range for most of the cell lines. These compounds also strongly interacted with BSA, as determined by UV-Visible and fluorescence spectroscopy. The binding constant values suggest that triazine-benzimidazole binds to the high affinity binding sites within albumin. From Forster non-radiative energy transfer equations, it has been found that the distance of compounds from BSA is in the range of 4-8 nm which predicts the possibility of energy transfer. The biological significance of this work is evident since the anticancer activity and the interaction of triazine-benzimidazole conjugates with albumin was not characterized earlier. Thus, triazine-benzimidazole studies clearly demonstrate that hybrids with heterocyclic hydrophobic groups are beneficial in biological and anticancer activity. These preliminary biological screening results offer encouragement and further mechanistic studies of these types of analogues are in progress.

4. Experimental section

4.1. Chemistry

All materials were obtained from commercial suppliers and used without further purification unless otherwise noted. Melting points were determined in open capillaries and were uncorrected. Reactions were monitored by thin-layer chromatography (TLC) carried out on silica gel plates (GF 254) using UV light as visualizing agents. ^{1}H NMR and ^{13}C NMR spectra were recorded on Jeol-400 (^{1}H, 400 MHz; ^{13}C, 100 MHz) spectrometer at ambient temperature, using $CDCl_3$, DMSO-d_6 and trifluoroacetic acid (TFA) as solvents. Chemical shifts are reported in parts per million (ppm) with TMS as an internal reference and *J* values are given in Hz. Mass spectrometric data were recorded at Waters Micromass Q-Tof Micro. Elemental analysis was done with Thermo Scientific (Flash 2000) analyzer. Hexane:ethyl acetate and chloroform:methanol were the adopted solvent systems. UV-Visible studies were carried out Shimadzu-2400 PC spectrometer. The fluorescence spectra were determined on a Varian Cary Eclipse fluorescence spectrometer.

*4.2. Synthesis of 4,6-dichloro-2-morpholin-4-yl-[1,3,5]triazine (**2**)*

To a stirred solution of cyanuric chloride (10 g, 0.054 mol) in anhydrous THF (150 mL), morpholine (5.65 g, 0.065 mol) was added at 0-5 ^{0}C. To this mixture, 10% $NaHCO_3$ was added and stirred at the same temperature for 6 h. The resulted reaction mixture was then poured into crushed ice, filtered, dried and column chromatographed on silica gel in hexane : ethylacetate to afford the desired product 4,6-dichloro-2-morpholin-4-yl-[1,3,5]triazine (**2**) as white solid; (11.33 g, 89%); mp: 277-279 ^{0}C [34].

*4.3. Synthesis of 4-(1H-benzimidazol-2-yl)-phenylamine (**3**)*

A mixture of 4-aminobenzoic acid (5 g, 5.78 mmol) and *o*-phenylenediamine (3.9 g, 3.68 mmol) were stirred in a syrupy polyphosphoric acid (12.5 gm) at 200 ^{0}C for 5 h. The reaction was monitored by TLC. The reaction mixture was cooled and poured into crushed ice. The white precipitate was then stirred in cold water. Ammonium hydroxide solution was added until the pH 7.0 was achieved. The resulting solid was filtered and washed several times with methanol and column chromatographed on silica gel in hexane : ethylacetate to afford the desired product 4-(1*H*-benzimidazol-2-yl)-phenylamine (**3**) as white solid; (82%); mp: 207-209 ^{o}C; ^{1}H NMR (400 MHz, DMSO-d_6): δ = 7.96 (d, 2H, *J* = 8.72 Hz, ArH), 7.55-7.51 (m, 2H, ArH), 7.16-7.14 (m, 2H, ArH), 6.75 (d, 2H, *J* = 8.24 Hz, ArH), 4.45 (bs, 2H, NH_2); ^{13}C NMR (100 MHz, $CDCl_3$ + DMSO-d_6): δ = 152.2, 148.4, 127.5, 120.9, 118.6, 113.8 (ArC); MS(ESI), m/z: 209.2 (M^++1).

*4.4. Synthesis of [4-(3H-benzimidazol-5-yl)-phenyl]-(6-chloro-2-morpholin-4-yl-[1,3,5]triazin-2-yl)-amine (**4**)*

To a stirred solution of 4,6-dichloro-2-morpholin-4-yl-[1,3,5]triazine (**2**) (10 g, 0.042 mol) in anhydrous THF (150 mL), 4-(1*H*-benzimidazol-2-yl)-phenylamine (**3**) (10.67 g, 0.051 mol) was added at room temperature. To this mixture, 10% K_2CO_3 was added and stirred for 24 h. The resulted reaction mixture was then poured into crushed ice, filtered, dried and column chromatographed on silica gel using hexane : ethylacetate to afford the desired product [4-(3*H*-benzimidazol-5-yl)-phenyl]-(6-chloro-2-morpholin-4-yl-[1,3,5]triazin-2-yl)-amine **(4)** as white solid; 84%; mp: 277-279 ^{o}C; ^{1}H NMR (400 MHz, $CDCl_3$ + DMSO-d_6): δ = 9.94 (bs, 1H, NH), 8.14 (d, 2H, *J* = 8.68 Hz, ArH), 7.81 (d, 2H, *J* = 8.72 Hz, ArH), 7.62-7.56 (m, 2H, ArH), 7.21-7.18 (m, 2H, ArH), 3.87-3.86 (m, 4H, mor-CH_2), 3.77-3.75 (m, 4H, mor-CH_2); ^{13}C NMR (100 MHz, $CDCl_3$): δ = 152.9, 142.8, 135.6, 129.1, 128.1, 126.2, 109.4 (ArC), 66.7 (O-CH_2), 47.3 (N-CH_2); MS(ESI), m/z: 409.5 (M^++2); Anal. Calcd for $C_{20}H_{18}ClN_7O$: C, 58.90; H, 4.45; N, 24.04, Found: C, 58.99; H, 4.41; N, 24.20.

*4.5. General procedure for the synthesis of compounds **5-15***

To a stirred solution of [4-(3*H*-benzimidazol-5-yl)-phenyl]-(6-chloro-2-morpholin-4-yl-[1,3,5]triazine-2,4-diamine **(4)** (0.200 g, 0.463 mmol) in 1,4-dioxane (20 mL), amine (0.556 mmol) and potassium carbonate (0.095g, 0.695 mmol) were added and heated at 110 ^{o}C for 8-12 h. Extracted the reaction mixture with chloroform, dried over Na_2SO_4, filtered and concentrated to get crude product which was then purified through column chromatography using chloroform:methanol (50:1) as eluents to give compounds **5-15**.

*4.5.1. [4-(3H-Benzimidazol-5-yl)-phenyl]-(2,6-di-morpholin-4-yl-[1,3,5]triazin-2-yl)-amine (**5**)*

White solid; yield: 78%; mp: 268-270 ^{o}C; ^{1}H NMR (400 MHz, $CDCl_3$): δ = 8.00 (d, 2H, *J* = 7.76 Hz, ArH), 7.70 (d, 3H, *J* = 8.24 Hz, ArH), 7.27-7.25 (m, 3H, ArH), 6.87 (bs, 1H, NH), 3.81-3.76 (m, 8H, mor-CH_2), 3.74-3.70 (m, 8H, mor-CH_2); ^{13}C NMR (100 MHz, $CDCl_3$): δ = 165.1, 151.6, 135.8, 129.2, 128.2, 128.0, 125.7, 118.9, 115.5, 101.1 (ArC), 66.8 (O-CH_2), 43.6 (N-CH_2); MS(ESI), m/z: 481.3 (M^++23); Anal. Calcd for $C_{24}H_{26}N_8O_2$: C, 62.87; H, 5.72; N, 24.44, Found: C, 62.98; H, 5.67; N, 24.55.

*4.5.2. [4-(3H-Benzimidazol-5-yl)-phenyl]-(2-morpholin-4-yl-6-piperidin-1-yl-[1,3,5]triazin-2-yl)-amine (**6**)*

White solid; yield: 72%; mp: 271-273 ^{o}C; ^{1}H NMR (400 MHz, $CDCl_3$): δ = 8.00 (d, 2H, *J* = 8.72 Hz, ArH), 7.72 (d, 2H, *J* = 8.72 Hz, ArH), 7.62 (s, 1H, ArH), 7.26-7.24 (m, 3H, ArH), 6.88 (bs, 1H, NH), 3.79 (t, 4H, *J* = 5.42 Hz, mor-CH_2), 3.75-3.68 (m, 8H, mor-CH_2, pip-CH_2), 1.68-1.59 (m, 6H, pip-CH_2); ^{13}C NMR (100 MHz, $CDCl_3$): δ = 152.3, 143.0, 135.9, 134.6, 131.4, 129.0, 127.9, 126.2, 116.1, 110.5, 109.0, (ArC), 67.0 (O-CH_2), 44.2 (N-CH_2), 43.7 (N-CH_2), 25.9 (CH_2), 25.0 (CH_2); MS(ESI), m/z: 479.5 (M^++23); Anal. Calcd for $C_{25}H_{28}N_8O$: C, 65.77; H, 6.18; N, 24.54, Found: C, 65.65; H, 6.14; N, 24.62.

*4.5.3. [4-(3H-Benzimidazol-5-yl)-phenyl]-(2-morpholin-4-yl-6-pyrrolidin-1-yl-[1,3,5]triazin-2-yl)-amine (**7**)*

White solid; yield: 76%; mp: 277-279 ^{o}C; ^{1}H NMR (400 MHz, $CDCl_3$): δ = 7.99 (d, 2H, *J* = 8.68 Hz, ArH), 7.75 (d, 2H, *J* = 8.68 Hz, ArH), 7.61 (bs, 1H, NH), 7.25-7.23 (m, 4H, ArH), 6.94 (bs, 1H, NH), 3.82-3.79 (m, 4H, mor-CH_2), 3.74-3.72 (m, 4H, mor-CH_2), 3.57 (t, 4H, *J* = 5.04 Hz, pyrr-CH_2), 1.96-1.94 (m, 4H, pyrr-CH_2); ^{13}C NMR (100 MHz, $CDCl_3$): δ = 152.2, 143.0, 136.0, 134.8, 129.0, 127.9, 126.2, 115.8, 110.3, 109.0 (ArC), 67.0 (O-CH_2), 46.1 (N-

CH_2), 43.7 (N-CH_2), 25.4 (CH_2); MS(ESI), m/z: 442.3 (M^+); Anal. Calcd for $C_{24}H_{26}N_8O$: C, 65.14; H, 5.92; N, 25.32, Found: C, 65.25; H, 5.88; N, 25.39.

*4.5.4. [4-(3H-Benzimidazol-5-yl)-phenyl]-[6-(4-methyl-piperazin-1-yl)-2-morpholin-4-yl-[1,3,5]triazin-2-yl]-amine (**8**)*

White solid; yield: 77%; mp: 282-284 ^oC; ^1H NMR (400 MHz, $CDCl_3$): δ = 8.01 (d, 2H, *J* = 8.72 Hz, ArH), 7.70 (d, 2H, *J* = 8.72 Hz, ArH), 7.63 (bs, 1H, NH), 7.27-7.24 (m, 4H, ArH), 6.87 (bs, 1H, NH), 3.84 (t, 4H, *J* = 4.12 Hz, mor-CH_2), 3.80-3.78 (m, 4H, mor-CH_2), 3.75-3.72 (m, 4H, piperazine-CH_2), 2.46 (t, 4H, *J* = 4.60 Hz, piperazine-CH_2), 2.35 (s, 3H, N-CH_3); ^{13}C NMR (100 MHz, $CDCl_3$): δ = 138.2, 135.9, 135.8, 135.1, 129.1, 127.9, 125.9, 118.9, 115.2, 100.8 (ArC), 66.8 (O-CH_2), 46.8 (N-CH_2), 44.2 (N-CH_2), 43.6 (N-CH_2), 14.0 (N-CH_3); MS(ESI), m/z: 471.5 (M^+); Anal. Calcd for $C_{25}H_{29}N_9O$: C, 63.68; H, 6.20; N, 26.73, Found: C, 63.79; H, 6.15; N, 26.66.

*4.5.5. N-[4-(3H-Benzimidazol-5-yl)-phenyl]-2-morpholin-4-yl-N'-(6-morpholin-4-yl-ethyl)-[1,3,5]triazine-4,6-diamine (**9**)*

White solid; yield: 69%; mp: 289-291 ^oC; ^1H NMR (400 MHz, $CDCl_3$): δ = 8.05 (s, 1H, ArH), 7.30 (t, 4H, *J* = 7.36 Hz, ArH, NH), 7.10 (d, 2H, *J* = 8.24 Hz, ArH), 7.05 (d, 2H, *J* = 11.36 Hz, ArH), 3.82-3.80 (m, 8H, mor-CH_2), 3.72-3.69 (m, 8H, mor-CH_2), 3.51-3.49 (m, 2H, N-CH_2), 2.20-2.17 (m, 2H, N-CH_2); ^{13}C NMR (100 MHz, $CDCl_3$): δ = 166.0, 164.6, 152.5, 142.9, 135.8, 129.1, 128.0, 126.3, 122.1, 121.7, 115.5, 115.2, 109.1 (ArC), 66.9 (O-CH_2), 57.2 (N-CH_2), 53.4 (N-CH_2), 47.2 (N-CH_2), 37.1 (N-CH_2); MS(ESI), m/z: 524.3 (M^++23); Anal. Calcd for $C_{26}H_{31}N_9O_2$: C, 62.26; H, 6.23; N, 25.13, Found: C, 62.30; H, 6.18; N, 25.25.

*4.5.6. 2-(4-{4-[4-(3H-Benzimidazol-5-yl)-phenylamino]-2-morpholin-4-yl-[1,3,5]triazin-6-yl}-piperazin-1-yl)-ethanol (**10**)*

White solid; yield: 68%; mp: 287-289 ^oC; ^1H NMR (400 MHz, $CDCl_3$): δ = 7.60 (d, 1H, *J* = 8.72 Hz, ArH), 7.33-7.27 (m, 3H, ArH), 7.17 (s, 1H, ArH), 7.08 (d, 1H, *J* = 8.72 Hz, ArH), 7.03 (d, 2H, *J* = 6.40 Hz, ArH), 3.67-3.57 (m, 12H, mor-CH_2, piperazine-CH_2), 3.47 (d, 2H, *J* = 8.28 Hz, O-CH_2), 2.43-2.42 (m, 2H, N-CH_2), 2.15-2.13 (m, 4H, piperazine-CH_2); ^{13}C NMR (100 MHz, $CDCl_3$): δ = 151.7, 138.4, 135.9, 135.8, 134.7, 129.1, 127.9, 125.9, 118.9, 115.7, 115.5 (ArC), 66.9 (O-CH_2), 66.7 (O-CH_2), 57.3 (N-CH_2), 53.4 (N-CH_2), 43.6 (N-CH_2), 36.9 (N-CH_2); MS(ESI), m/z: 501.3 (M^+); Anal. Calcd for $C_{26}H_{31}N_9O_2$: C, 62.26; H, 6.23; N, 25.13, Found: C, 62.15; H, 6.18; N, 25.24.

*4.5.7. N-(6-Amino-ethyl)-N'-[4-(3H-benzimidazol-5-yl)-phenyl]-2-morpholin-4-yl-[1,3,5]triazine-4,6-diamine (**11**)*

White solid; yield: 73%; mp: 265-267 ^{o}C; ^{1}H NMR (400 MHz, $CDCl_3$): δ = 7.95 (d, 2H, *J* = 7.76 Hz, ArH), 7.62-7.59 (m, 4H, ArH, NH), 7.25-7.22 (m, 3H, ArH), 3.75-3.73 (m, 4H, mor-CH_2), 3.71-3.67 (m, 4H, mor-CH_2), 3.46 (t, 2H, *J* = 5.96 Hz, N-CH_2), 2.91 (t, 2H, *J* = 5.48 Hz, N-CH_2); ^{13}C NMR (100 MHz, $CDCl_3$): δ = 152.4, 143.0, 135.9, 134.2, 131.7, 129.1, 128.0, 126.2, 109.1 (ArC), 66.9 (O-CH_2), 47.2 (N-CH_2), 43.7 (N-CH_2), 41.8 (N-CH_2); MS(ESI), m/z: 431.3 (M^+); Anal. Calcd for $C_{22}H_{25}N_9O$: C, 61.24; H, 5.84; N, 29.21, Found: C, 61.39; H, 5.80; N, 29.14.

*4.5.8. 2-{4-[4-(3H-Benzimidazol-5-yl)-phenylamino]-2-morpholin-4-yl-[1,3,5]triazin-6-ylamino}-ethanol (**12**)*

White solid; yield: 71%; mp: 262-264 ^{o}C; ^{1}H NMR (400 MHz, $CDCl_3$): δ = 8.05 (s, 1H, ArH), 7.31 (d, 3H, *J* = 7.36 Hz, ArH), 7.24-7.22 (m, 1H, ArH), 7.11 (d, 1H, *J* = 8.24 Hz, ArH), 7.05 (d, 2H, *J* = 6.88 Hz, ArH), 3.79-3.72 (m, 8H, mor-CH_2), 3.49 (t, 2H, *J* = 5.48 Hz, O-CH_2), 2.91-2.88 (m, 2H, N-CH_2); ^{13}C NMR (100 MHz, $CDCl_3$): δ = 152.5, 142.8, 135.8, 133.9, 131.8, 129.1, 128.0, 126.2, 116.6, 111.4, 109.1 (ArC), 66.8 (O-CH_2), 63.8 (O-CH_2), 47.2 (N-CH_2), 43.7 (N-CH_2); MS(ESI), m/z: 455.9 (M^++23); Anal. Calcd for $C_{22}H_{24}N_8O_2$: C, 61.10; H, 5.59; N, 25.91, Found: C, 61.01; H, 5.55; N, 25.99.

*4.5.9. N-[4-(3H-Benzimidazol-5-yl)-phenyl]-N'-benzyl-2-morpholin-4-yl-[1,3,5]triazine-4,6-diamine (**13**)*

White solid; yield: 66%; mp: 275-277 ^{o}C; ^{1}H NMR (400 MHz, $CDCl_3$): δ = 8.04 (d, 1H, *J* = 1.80 Hz, ArH), 7.30-7.27 (m, 4H, ArH), 7.24 (d, 1H, *J* = 1.80 Hz, ArH), 7.22 (d, 1H, *J* = 2.28 Hz, ArH), 7.11 (d, 2H, *J* = 8.72 Hz, ArH), 7.05 (d, 2H, *J* = 1.84 Hz, ArH), 7.03 (d, 2H, *J* = 4.12 Hz, ArH), 5.28 (s, 2H, N-CH_2), 3.72 (t, 8H, *J* = 8.72 Hz, mor-CH_2); ^{13}C NMR (100 MHz, $CDCl_3$): δ = 151.9, 138.8, 135.8, 134.9, 134.0, 129.1, 128.0, 126.0, 122.1, 119.1, 115.5, 115.3, 101.7 (ArC), 66.7 (O-CH_2), 46.9 (N-CH_2), 43.7 (N-CH_2); MS(ESI), m/z: 478.3 (M^+); Anal. Calcd for $C_{27}H_{26}N_8O$: C, 67.77; H, 5.48; N, 23.42, Found: C, 67.71; H, 5.43; N, 23.49.

*4.5.10. N-[4-(3H-Benzimidazol-5-yl)-phenyl]-N'-cyclohexyl-2-morpholin-4-yl-[1,3,5]triazine-4,6-diamine (**14**)*

White solid; yield: 68%; mp: 283-285 ^{o}C; ^{1}H NMR (400 MHz, $CDCl_3$): δ = 8.00 (d, 2H, *J* = 7.76 Hz, ArH), 7.76 (d, 1H, *J* = 6.88 Hz, ArH), 7.67-7.62 (m, 2H, ArH), 7.25-7.23 (m, 2H,

ArH), 6.95 (s, 1H, ArH), 4.95 (m, 1H, N-CH), 3.79-3.73 (m, 8H, mor-CH_2), 2.05-2.02 (m, 2H, CH_2), 1.77-1.74 (m, 2H, CH_2), 1.66-1.64 (m, 2H, CH_2), 1.41-1.38 (m, 2H, CH_2), 1.25-1.19 (m, 2H, CH_2); ^{13}C NMR (100 MHz, $CDCl_3$): δ = 165.8, 164.4, 152.0, 151.9, 135.9, 135.7, 129.0, 127.9, 126.3, 126.1, 119.0, 115.5, 115.3 (ArC), 66.9 (O-CH_2), 57.2 (N-CH), 53.4 (N-CH_2), 37.1 (CH_2), 32.0 (CH_2), 22.7 (CH_2); MS(ESI), m/z: 471.3 (M^++1); Anal. Calcd for $C_{26}H_{30}N_8O$: C, 66.36; H, 6.43; N, 23.81, Found: C, 66.48; H, 6.38; N, 23.89.

*4.5.11. [4-(3H-Benzimidazol-5-yl)-phenyl]-(6-hydrazino-2-morpholin-4-yl-[1,3,5]triazin-4-yl)-amine (**15**)*

White solid; yield: 64%; mp: 296-298 ^{o}C; ^{1}H NMR (400 MHz, $CDCl_3$): δ = 7.67 (d, 1H, *J* = 8.60 Hz, ArH), 7.61 (d, 1H, *J* = 8.72 Hz, ArH), 7.48 (bs, 1H, NH), 7.25-7.23 (m, 2H, ArH), 7.11-6.98 (m, 4H, ArH), 3.67-3.65 (m, 4H, mor-CH_2), 3.50-3.47 (m, 4H, mor-CH_2); ^{13}C NMR (100 MHz, $CDCl_3$): δ = 152.4, 139.4, 135.6, 132.8, 129.2, 128.1, 125.7, 119.2, 116.2, 102.1 (ArC), 66.6 (O-CH_2), 43.9 (N-CH_2); MS(ESI), m/z: 403.7 (M^+); Anal. Calcd for $C_{20}H_{21}N_9O$: C, 59.54; H, 5.25; N, 31.25, Found: C, 59.64; H, 5.21; N, 31.28.

*4.6. General procedure for the synthesis of compounds **16-21***

To a stirred solution of [4-(3*H*-benzimidazol-5-yl)-phenyl]-(6-chloro-2-morpholin-4-yl-[1,3,5]triazin-2-yl)-amine **(4)** (0.200 g, 0.490 mmol) in 1,4-dioxane (20 mL), arylboronic acids (0.556 mmol), $Pd(PPh_3)_4$ (10 mol%) and potassium carbonate (0.101g, 0.736 mmol) were added and refluxed for 8-10 h in an inert atmosphere. After the completion of reaction, extracted the reaction mixture with chloroform, dried over Na_2SO_4, filtered and concentrated to get crude product which was purified through column chromatography using chloroform:methanol (50:1) as eluents to give compounds **16**-**21**.

*4.6.1. [4-(3H-Benzimidazol-5-yl)-phenyl]-(2-morpholin-4-yl-6-phenyl-[1,3,5]triazin-2-yl)-amine (**16**)*

White solid; yield: 72%; mp: 267-269 ^{o}C; ^{1}H NMR (400 MHz, $CDCl_3$): δ = 8.06 (d, 1H, *J* = 8.72 Hz, ArH), 8.00 (d, 1H, *J* = 4.68 Hz, ArH), 7.85 (d, 1H, *J* = 8.24 Hz, ArH), 7.77 (d, 1H, *J* = 8.96 Hz, ArH), 7.72 (d, 2H, *J* = 8.72 Hz, ArH), 7.62 (bs, 1H, NH), 7.54-7.52 (m, 3H, ArH), 7.08 (t, 2H, *J* = 8.72 Hz, ArH), 6.77-6.70 (m, 2H, ArH), 3.99-3.95 (m, 8H, mor-CH_2); ^{13}C NMR (100 MHz, $CDCl_3$): δ = 152.0, 137.6, 135.8, 134.0, 132.1, 129.7, 129.2, 128.6, 128.5, 128.0, 125.8, 119.2, 115.7, 101.5 (ArC), 66.8 (O-CH_2), 43.7 (N-CH_2); MS(ESI), m/z: 472.6 (M^++23); Anal. Calcd for $C_{26}H_{23}N_7O$: C, 69.47; H, 5.16; N, 21.81, Found: C, 69.64; H, 5.12; N, 21.98.

*4.6.2. [4-(3H-Benzimidazol-5-yl)-phenyl]-[6-(4-fluoro-phenyl)-2-morpholin-4-yl-[1,3,5]triazin-2-yl]-amine (**17**)*

White solid; yield: 71%; mp: 279-281 ^{o}C; ^{1}H NMR (400 MHz, $CDCl_3$): δ = 8.34 (d, 2H, *J* = 7.32 Hz, ArH), 8.03 (bs, 1H, NH), 7.67 (d, 1H, *J* = 8.28 Hz, ArH), 7.48 (d, 1H, *J* = 7.32 Hz, ArH), 7.40-7.37 (m, 2H, ArH), 7.35-7.29 (m, 3H, ArH), 7.16 (d, 1H, *J* = 2.32 Hz, ArH), 7.07 (d, 2H, *J* = 6.40 Hz, ArH), 3.98-3.61 (m, 8H, mor-CH_2); ^{13}C NMR (100 MHz, $CDCl_3$): δ = 151.9, 138.8, 135.8, 134.9, 134.0, 129.1, 128.0, 126.0, 122.1, 119.1, 115.5, 115.3, 101.7 (ArC), 66.7 (O-CH_2), 43.7 (N-CH_2); MS(ESI), m/z: 467.3 (M^+); Anal. Calcd for $C_{26}H_{22}FN_7O$: C, 66.80; H, 4.74; N, 20.97, Found: C, 66.85; H, 4.71; N, 21.05.

*4.6.3. [4-(3H-Benzimidazol-5-yl)-phenyl]-(6-furan-2-yl-2-morpholin-4-yl-[1,3,5]triazin-4-yl)-amine (**18**)*

White solid; yield: 66%; mp: 282-284 ^{o}C; ^{1}H NMR (400 MHz, $CDCl_3$): δ = 8.00 (d, 2H, *J* = 4.72 Hz, ArH), 7.83 (bs, 1H, NH), 7.72 (d, 2H, *J* = 8.24 Hz, ArH), 7.52-7.48 (m, 3H, ArH), 7.07 (t, 3H, *J* = 8.68 Hz, ArH), 6.96 (s, 1H, ArH), 6.80 (bs, 1H, NH), 3.77-3.69 (m, 8H, mor-CH_2); ^{13}C NMR (100 MHz, $CDCl_3$): δ = 152.9, 142.8, 135.6, 132.5, 129.1, 128.1, 126.2, 109.4 (ArC), 66.7 (O-CH_2), 44.1 (N-CH_2); MS(ESI), m/z: 439.2 (M^+); Anal. Calcd for $C_{24}H_{21}N_7O_2$: C, 65.59; H, 4.82; N, 22.31, Found: C, 65.86; H, 4.87; N, 22.39.

*4.6.4. 4-(3H-Benzimidazol-5-yl)-phenyl]-(2-morpholin-4-yl-6-thiophen-2-yl-[1,3,5]triazin-2-yl)-amine (**19**)*

White solid; yield: 67%; mp: 288-290 ^{o}C; ^{1}H NMR (400 MHz, $CDCl_3$): δ = 7.50 (q, 3H, *J* = 5.04 Hz, ArH), 7.37-7.31 (m, 3H, ArH), 7.14 (d, 2H, *J* = 5.96 Hz, ArH), 7.03 (t, 3H, *J* = 8.72 Hz, ArH), 6.86 (bs, 1H, NH), 3.79-3.78 (m, 4H, mor-CH_2), 3.75-3.74 (m, 4H, mor-CH_2); ^{13}C NMR (100 MHz, $CDCl_3$): δ = 152.6, 143.0, 135.8, 135.1, 133.6, 132.0, 129.1, 128.0, 126.2, 121.7, 115.5, 115.3, 109.1 (ArC), 66.9 (O-CH_2), 43.8 (N-CH_2); MS(ESI), m/z: 478.3 (M^++23); Anal. Calcd for $C_{24}H_{21}N_7OS$: C, 63.28; H, 4.65; N, 21.52; S, 7.04, Found: C, 63.15; H, 4.61; N, 21.59; S, 7.08.

*4.6.5. [4-(3H-Benzimidazol-5-yl)-phenyl]-[6-(4-chloro-phenyl)-2-morpholin-4-yl-[1,3,5]triazin-2-yl]-amine (**20**)*

White solid; yield: 68%; mp: 276-278 ^{o}C; ^{1}H NMR (400 MHz, $CDCl_3$): δ = 8.35 (d, 2H, *J* = 5.48 Hz, ArH), 8.01 (bs, 1H, NH), 7.67 (d, 1H, *J* = 8.24 Hz, ArH), 7.33-7.31 (m, 4H, ArH), 7.16 (d, 2H, *J* = 8.68 Hz, ArH), 7.07 (d, 3H, *J* = 5.96 Hz, ArH), 3.99-3.73 (m, 8H, mor-CH_2); ^{13}C NMR (100 MHz, $CDCl_3$): δ = 152.4, 139.4, 135.6, 132.8, 129.2, 128.1, 125.7, 119.2,

116.2, 102.1 (ArC), 66.6 (O-CH_2), 43.9 (N-CH_2); MS(ESI), m/z: 484.3 (M^++1); Anal. Calcd for $C_{26}H_{22}ClN_7O$: C, 64.53; H, 4.58; N, 20.26, Found: C, 64.64; H, 4.41; N, 20.31.

*4.6.6. [4-(3H-Benzimidazol-5-yl)-phenyl]-[6-(4-trifluoromethyl-phenyl)-2-morpholin-4-yl-[1,3,5]triazin-2-yl]-amine (**21**)*

White solid; yield: 65%; mp: 279-281 ^oC; ^1H NMR (400 MHz, $CDCl_3$): δ = 8.03 (s, 1H, ArH), 7.50-7.46 (m, 2H, ArH), 7.31-7.28 (m, 2H, ArH), 7.24-7.22 (m, 2H, ArH), 7.13 (d, 1H, *J* = 8.72 Hz, ArH), 7.06 (d, 2H, *J* = 6.88 Hz, ArH), 6.99-6.97 (m, 2H, ArH), 6.86 (bs, 1H, NH), 3.81-3.78 (m, 4H, mor-CH_2), 3.74-3.71 (m, 4H, mor-CH_2); ^{13}C NMR (100 MHz, $CDCl_3$): δ = 152.0, 138.7, 136.8, 135.8, 134.1, 131.6, 129.6, 129.2, 128.3, 128.0, 125.9, 119.1, 115.6, 101.4 (ArC), 66.8 (O-CH_2), 43.7 (N-CH_2); MS(ESI), m/z: 517.3 (M^+); Anal. Calcd for $C_{27}H_{22}F_3N_7O$: C, 62.66; H, 4.28; N, 18.95, Found: C, 67.59; H, 4.18; N, 18.85.

4.7. Procedure for in vitro anticancer screening

The human tumor cell lines of cancer screening were grown in RPMI 1640 medium containing 5% fetal bovine serum and 2 mM L-glutamine. Cells were inoculated in 96 well plates in 100 µL per well at plating densities ranging from 5,000 to 40,000 cells/well that depends upon the doubling time of individual cell lines. The microtiter plates were then incubated at 37 °C, 95% air, 5% CO_2, and 100% relative humidity for 24 h. Two plates of each cell line were then fixed *in situ* with TCA. Experimental drugs were dissolved in DMSO at 400-fold the desired final maximum test concentration and stored frozen prior to use. At the time of drug addition, an aliquot of frozen concentrate was used and diluted to two times the desired final maximum test concentration with complete medium containing 50 µg/ml gentamicin. Additional four, 10-fold or ½ log serial dilutions were made to give total of five drug concentrations plus control. Aliquots of 100 µL of these drug dilutions were added to the appropriate microtiter wells. Following the addition, plates were incubated at 37 °C, 5% CO_2, 95% air, and 100% relative humidity for 48 h. For adherent cells, the assay was terminated by the addition of cold TCA. Cells were fixed *in situ* by the addition of 50 µL of cold 50% (w/v) TCA and incubated at 4 °C for 60 min. The plates were washed five times with tap water by discarding the supernatant and air dried. Sulforhodamine B (SRB) solution (100 µL) at 0.4% (w/v) in 1% acetic acid was added to each well followed by incubation of plates for 10 min at room temperature. After staining, unbound dye was removed by washing five times with 1% acetic acid and the plates were air dried before subsequent solubilization with 10 mM trizma base. The absorbance was read at a wavelength of 515 nm on an

automated plate reader. With seven absorbance measurements [time zero (T_z), control growth (C), and test growth in the presence of drug at five concentration levels (T_i)], percentage growth was calculated at each of the drug concentration levels. Percentage growth inhibition was calculated as:

[(Ti -Tz)/(C - Tz)] × 100 for concentrations for which $T_i \geq Tz$; [(Ti -Tz)/Tz] × 100 for concentrations for which Ti < Tz.

Three dose response parameters were calculated for each experimental agent. Growth inhibition of 50% (GI_{50}) was calculated from [(Ti -Tz)/(C - Tz)] × 100 = 50. Drug concentration resulting in total growth inhibition (TGI) was calculated from T_i = Tz. LC_{50} was calculated from [(Ti-Tz)/Tz]×100 = 50

4.8. Procedure for BSA screening

4.8.1. *Materials and methods*

The stock solution of BSA (Sigma Chemical Co., USA) was prepared by dissolving an appropriate amount of solid BSA in 0.1 M phosphate buffer at pH 7.4 and stored at 0−4 °C in the dark. Stock solutions of compounds **5-21** (10^{-3} mol L^{-1}) were prepared in DMSO. All stock solutions were diluted to the required concentrations with phosphate buffer (pH 7.4). All other reagents were of analytical reagent grade.

4.8.2. UV-Visible absorption and fluorescence spectra

UV-visible absorption and fluorescence emission spectra were measured with a 1 cm quartz cell. All the spectra were recorded at ambient temperature (300 K). UV-Vis spectra were recorded on Shimadzu-2400 PC spectrometer. The wavelength of the spectra was between 200 and 800 nm. All the UV-visible spectra were recorded after equilibration of solution for 5 min. Emission spectra were recorded with Varian Cary Eclipse fluorescence spectrometer. The excitation and emission wavelengths for BSA were 280 nm and 351 nm with a slit width of 10 nm. Very dilute solutions of BSA and compounds **5-21** were used to avoid inner filter effect. The titration experiments were performed by varying the concentration of compounds **5-21** and keeping the BSA concentration (10 μM).

Binding constant K was estimated from absorption and fluorescence titration data using the Benesi–Hildebrand equation. K was determined from the ratio of intercept to slope obtained from the linear fit of the plot of $1/(A_0 - A)$ vs. 1/[compound] and $1/(F_0 - F)$ vs.

1/[compound], where A_0 and A are the absorption intensities and F_0 and F are the emission intensities of the BSA in the absence and presence of compounds, respectively.

$$1/(A_0 - A) = 1/(A_0 - A_{fc}) + \{1/[K(A_0 - A_{fc})]\}[ligand]$$

To determine the binding number of triazine-benzimidazole analogues with BSA, the double-logarithmic equation was used:

$$\log[(F_0\text{-}F)/F] = \log K + n \log [Q]$$

where, F_0 and F are the emission intensities of BSA in the absence and presence of triazine-benzimidazole analogues, respectively. A plot of $\log[(F_0\text{-}F)/F]$ vs. $\log[Q]$ will produce a straight line; whose slope is equal to n. The number of binding sites n as calculated from the plot is approximately equal to 1 for BSA and it is in good agreement with the literature reports.

Acknowledgments

KP thanks the Department of Science and Technology, New Delhi (EMR/2014/000669). PS is grateful for a DST/Inspire Fellowship (Fellow Code-IF110542). NCI, NIH, USA was greatly acknowledged for anticancer activities.

Abbreviations

BSA, bovine serum albumin; Trp-134 and Trp-212, tryptophan residues; NCI, National Cancer Institution, CNS, central nervous system; GI %, percentage growth inhibition; GI_{50}, 50 % growth inhibition; TGI, total growth inhibition; LC_{50}, 50 % lethal concentration; MG-MID, mean graph midpoints; Trp, tryptophan; Tyr, tyrosine; Phe, phenylalanine; UV-Vis., ultraviolet visible; FRET, fluorescence resonance energy transfer; *K*, binding constant; n, number of binding site, E, efficiency of energy transfer; R_0, critical distance; K^2, orientation factor; *n*, refractive index; Φ, quantum yield; *J*, degree of spectral overlap; THF, tetrahydrofuran; TLC, thin layer chromatography.

Notes and References

[1] http://www.cancer.gov.

[2] A.D. Kinghorn, Y.-W. Chin, S.M. Swanson, Curr. Opin. Drug Discov. Devel. 12 (2009) 189-196.

[3] P. Singla, V. Luxami, K. Paul, Eur. J. Med. Chem. 102 (2015) 39-57.

[4] P. Singla, V. Luxami, K. Paul, RSC Adv. 4 (2014) 12422-12440.

[5] (a) P. Singla, V. Luxami, K. Paul, Bioorg. Med. Chem. 23 (2015) 1691-1700. (b) P.

Singla, V. Luxami, K. Paul, Bioorg. Med. Chem. Lett. 26 (2016), 518-523.

[6] (a) A.L. Smith, N.D. D'Angelo, Y.Y. Bo, S.K. Booker, V.J. Cee, B. Herberich, F.T. Hong, C.L.M. Jackson, B.A. Lanman, L. Liu, N. Nishimura, L.H. Pettus, A.B. Reed, S. Tadesse, N.A. Tamayo, R.P. Wurz, K. Yang, K.L. Andrews, D.A. Whittington, J.D. McCarter, T.S. Miguel, L. Zalameda, J. Jiang, R. Subramanian, E.L. Mullady, S. Caenepeel, D.J. Freeman, L. Wang, N. Zhang, T. Wu, P.E. Hughes, M.H. Norman, J. Med. Chem. 55 (2012) 5188-5219. (b) M.H. Norman, K.L. Andrews, Y.Y. Bo, S.K. Booker, S. Caenepeel, V.J. Cee, N.D. D'Angelo, D.J. Freeman, B.J. Herberich, F.T. Hong, C.L.M. Jackson, J. Jiang, B.A. Lanman, L. Liu, J.D. McCarter, E.L. Mullady, N. Nishimura, L.H. Pettus, A.B. Reed, T.S. Miguel, A.L. Smith, M.M. Stec, S. Tadesse, A. Tasker, D. Aidasani, X. Zhu, R. Subramanian, N.A. Tamayo, L. Wang, D.A. Whittington, B. Wu, T. Wu, R.P. Wurz, K. Yang, L. Zalameda, N. Zhang, P.E. Hughes, J. Med. Chem. 55 (2012) 7796-7816. (c) R.P. Wurz, L. Liu, K. Yang, N. Nishimura, Y. Bo, L.H. Pettus, S. Caenepeel, D.J. Freeman, J.D. McCarter, E.L. Mullady, T.S. Miguel, L. Wang, N. Zhang, K.L. Andrews, D.A. Whittington, J. Jiang, R. Subramanian, P.E. Hughes, M.H. Norman, Bioorg. Med. Chem. Lett. 22 (2012) 5714-5720.

[7] (a) N. Busto, J. Valladolid, M.M. Alonso, H.J. Lozano, F.A. Jalón, B.R. Manzano, A.M. Rodríguez, M.C. Carrión, T. Biver, J.M. Leal, G. Espino, B. García, Inorg. Chem. 52 (2013) 9962-9974. (b) K. Arya, A. Dandia, Bioorg. Med. Chem. Lett. 17 (2007) 3298-3304. (c) G.W. Rewcastle, S.A. Gamage, J.U. Flanagan, R. Frederick, W.A. Denny, B.C. Baguley, P. Kestell, R. Singh, J.D. Kendall, E.S. Marshall, C.L. Lill, W.-J. Lee, S. Kolekar, C.M. Buchanan, S.M.F. Jamieson, P.R. Shepherd, J. Med. Chem. 54 (2011) 7105-7126.

[8] M. Koh, J.-C. Lee, C. Min, A. Moon, Bioorg. Med. Chem. 21 (2013) 2305-2313.

[9] S. Nozaki, M. Maeda, H. Tsuda, G.W. Sledge Jr., Breast Cancer Res. Treat. 83 (2004) 195-199.

[10] P.L. Rosee, T. Jia, S. Demehri, N. Hartel, P. deVries, L. Bonham, D. Hollenback, J.W. Singer, J.V. Melo, B.J. Druker, M.W. Deininger, Clin. Cancer Res. 12 (2006) 6540-6546.

[11] C.R. Lee, D. Faulds, Drugs 49 (1995) 932-953.

[12] R. Mallon, L.R. Feldberg, J. Lucas, I. Chaudhary, C. Dehnhardt, E.D. Santos, Z. Chen, O. dos Santos, S. Ayral-Kaloustian, A. Venkatesan, I. Hollander, Clin. Cancer Res. 17 (2011) 3193-3203.

[13] H. Peng, Z. Dong, J. Qi, Y. Yang, Y. Liu, Z. Li, J. Xu, J.T. Zhang, PLoS One 4 (2009) e5676-e5685.

[14] Y. Iino, T. Karakida, N. Sugamata, T. Andoh, H. Takei, M. Takahashi, S. Yaguchi, T. Matsuno, M. Takehara, M. Sakato, S. Kawashima, Y. Morishita, Anticancer Res. 18 (1998) 171-176.

[15] (a) R. Haaq, F. Kratz, Angew. Chem. Int. Ed. 45 (2006) 1198-1215. (b) S.E.A. Gratton, P.A. Ropp, P.D. Pohlhaus, J.C. Luft, V.J. Madden, M.E. Napier, JM. DeSimone, Proc. Natl. Acad. Sci. U.S.A. 105 (2008) 11613-11618.

[16] C.V. Kumar, A. Buranaprapuk, Angew. Chem. Int. Ed. Engl. 36 (1997) 2085-2087.

[17] F. Kratz, J. Controll. Release 132 (2008) 171-183.

[18] B. Elsadek, F. Kratz, J. Controll. Release 157 (2012) 4-28.

[19] F. Kratz, B. Elsadek, J. Controll. Release 161 (2012) 429-445.

[20] (a) T. Peters Jr., Adv. Protein Chem. 37 (1985) 161-245. (b) N. Tayeh, T. Rungassamy, J.R. Albani, J. Pharm. Biomed. Anal. 50 (2009) 107-116.

[21] Developmental Therapeutics Program, NCI/NIH. www.dtp.nci.nih.gov.

[22] M.R. Grever, S.A. Sehepartz, B.A. Chabners, Semin. Oncol. 19 (1992) 622-638.

[23] A. Monks, D. Schudiero, P. Skehan, R. Shoemaker, K. Paull, D. Vistica, C. Hose, J. Langley, P. Cronise, A. Vaigro-Wolff, M. Gray-Goodrich, H. Campbell, J. Mayo, M. Boyd, J. Natl. Cancer Inst. 83 (1991) 757-766.

[24] M.R. Boyd, K.D. Paull, Drug Dev. Res. 34 (1995) 91-109.

[25] H.A. Benesi, J.H. Hildebrand, J. Am. Chem. Soc. 71 (1949) 2703-2707.

[26] Y.-J. Hu, Y. Liu, X.H. Xiao, Biomacromolecules 10 (2009) 517-521.

[27] F.-F. Tian, F.-L. Jiang, X.-L. Han, C. Xiang, Y.-S. Ge, J.-H. Li, Y. Zhang, R. Li, X.-L. Ding, Y. Liu, J. Phys. Chem. B 114 (2010) 14842-14853.

[28] T. Forster, Ann. Phys. 437 (1948) 55-75.

[29] T. Forster, Discuss. Faraday Soc. 27 (1959) 7-17.

[30] J.R. Lakowicz, Principles of Fluorescence Spectroscopy, Kluwer Academic/Plenum Publishers, Dordrecht, The Netherlands (2004).

[31] X. Pan, P. Qin, R. Liu, J. Wang, J. Agric. Food Chem. 59 (2011) 6650-6656.

[32] G. Vignesh, S. Arunachalam, S. Vignesh, R.A. James, Spectrochim. Acta A, 96 (2012) 108-116.

[33] B. Valeur, J.C. Brochon, New Trends in Fluorescence spectroscopy, Springer, Berlin (2001).

[34] P.T. Selvam, P.P. Radhika, S. Janagaraj, A.S. Kumar, Res. Biotech., 2 (2011) 50-57.

Figures Captions

Figure 1. Triazines possessing anticancer activity.

Figure 2. Absorption spectral changes of BSA (10 μM) in phosphate buffer upon addition of compounds **6** (a), **16** (b), **17** (c) and **20** (d) at 0-20 μM; Insets indicate Benesi–Hildebrand plot of $1/[A_0\text{-}A]$ vs. 1/[compounds] for binding of BSA with compounds **6** (a)**, 16** (b), **17** (c) and **20** (d) through absorption spectral titrations.

Figure 3. Fluorescence spectral changes of BSA (10 μM) in phosphate buffer upon addition of **6** (a), **16** (b), **17** (c) and **20** (d) at 0-20 μM. Insets indicate Benesi–Hildebrand plot of $1/[F_0\text{-}F]$ vs. 1/[compounds] for binding of BSA with compounds **6** (a), **16** (b), **17** (c) and **20** (d) through emission spectral titrations.

Figure 4. Overlap of the fluorescence emission spectra of BSA with UV-Visible absorption spectra of compounds **6** (a), **16** (b), **17** (c) and **20** (d).

Scheme 1. Synthesis of triazine-benzmidazoles

Table 1. Effects of 10 μM of compounds **6, 16, 17** and **20** on cell proliferation in a subpanel tumor cell lines**.**

Table 2. Compounds **6, 16, 17** and **20** with median growth inhibitory (GI_{50}, μM), total growth inhibitory (TGI, μM) and median lethal concentrations (LC_{50}, μM) of *in vitro* tumor cell lines at five different concentrations viz., 10^{-4}, 10^{-5}, 10^{-6}, 10^{-7} and 10^{-8} M

Table 3. Photophysical properties and binding constants of BSA with compounds **5-14**, **16**, **17** and **20**.

Table 4. Forster energy transfer parameters for BSA and triazine-benzimidazoles (**5-14**, **16**, **17** and **20**).

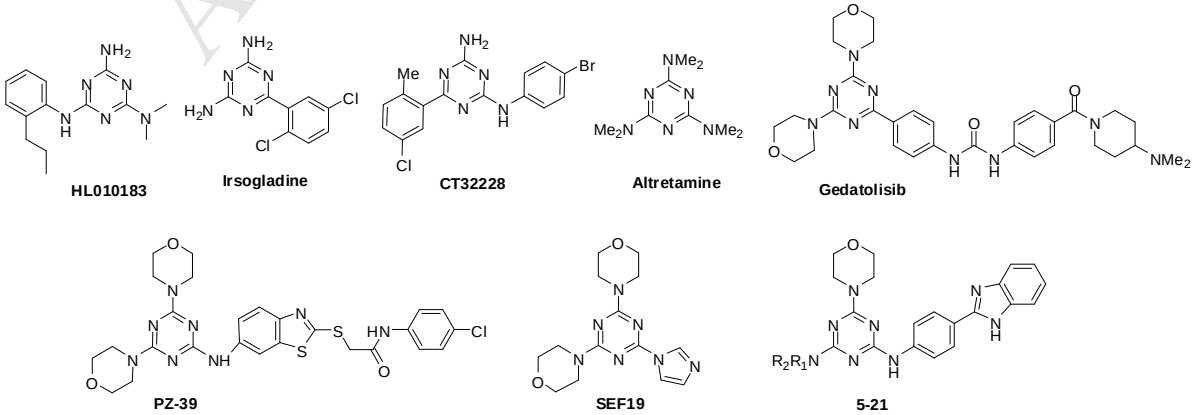

Figure 1. Triazines possessing anticancer activity.

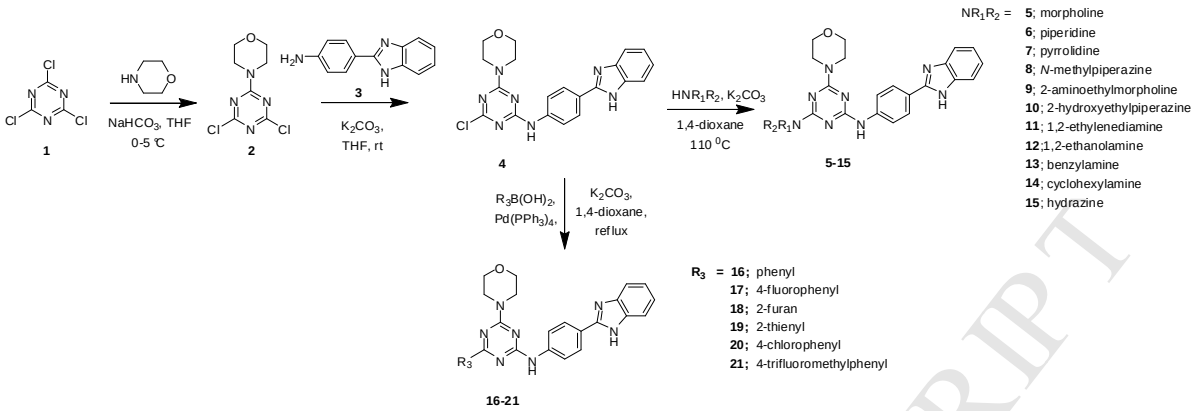

Scheme 1. Synthesis of triazine-benzmidazoles

Table 1. Effects of 10 μM of compounds **6, 16, 17** and **20** on cell proliferation in a subpanel tumor cell lines**.**

Subpanel tumor cell lines	6	16	17	20
Leukemia				
CCRF-CEM	8.74	-15.74	-1.84	-91.49
HL-60(TB)	-22.74	-32.69	-46.01	-81.44
K-562	-6.74	-30.14	-22.02	-100.0
MOLT-4	13.72	-37.78	1.78	-91.61
RPMI-8226	2.47	-22.64	-13.83	-73.43
SR	9.79	8.94	6.01	-83.32
Non-small cell lung cancer				
A549/ATCC	13.89	-68.45	11.23	-75.19
EKVX	27.70	-66.92	7.91	-91.35
HOP-62	-45.21	-64.49	-27.31	-73.89
HOP-92	43.35	-66.25	6.57	-72.10
NCI-H226	32.70	-19.29	17.11	-64.52
NCI-H23	19.72	-59.05	11.34	-83.39
NCI-H322M	35.03	-0.47	27.03	-92.85
NCI-H460	0.81	-67.25	0.13	-80.31
NCI-H522	9.25	-68.19	11.94	-73.93
Colon cancer				
COLO 205	-61.28	-68.80	-43.73	-68.39
HCC-2998	-1.07	-80.71	-19.85	-89.86
SF-295	-51.43	-76.36	-63.50	-94.37
SF-539	7.95	-76.83	0.31	-92.73
SNB-19	10.38	-18.63	17.47	-81.19
SNB-75	-0.68	-89.65	-19.21	-92.64
U251	8.02	-67.51	6.38	-93.05
Melanoma				
LOX IMVI	-77.07	-88.99	-75.60	-92.98
MALME-3M	-50.20	-77.26	-65.73	-73.43
M14	-24.53	-80.66	-7.64	-82.62
MDA-MB-435	-27.26	-81.06	-38.01	-86.10
SK-MEL-2	-20.55	-52.66	-19.20	-71.35
SK-MEL-28	-30.22	-82.85	-34.04	-84.68
SK-MEL-5	-90.75	-95.41	-90.65	-97.59

UACC-257	-19.30	-56.40	-27.63	-82.52
Ovarian cancer				
IGORV1	51.34	-38.08	33.68	-71.16
OVCAR-3	10.91	-73.44	5.15	-95.58
OVCAR-4	61.19	-47.23	59.84	-73.91
OVCAR-5	73.94	0.63	66.34	-74.72
OVCAR-8	45.70	-50.44	39.24	-73.82
NCI/ADR- RES	45.64	-60.81	34.23	-87.53
SK-OV-3	22.49	-30.32	19.61	-89.89
Renal cancer				
786-0	-57.34	-88.93	-60.02	-94.51
A498	-28.59	-83.40	-32.12	-81.51
ACHN	22.92	-58.90	9.00	-90.60
CAKI-1	-46.89	-89.38	-56.60	-93.57
RXF 393	-56.14	-75.14	-67.46	-91.12
SN12C	52.41	-62.79	40.78	-79.48
TK-10	58.80	-58.06	43.87	-94.44
UO-31	-37.82	-60.57	-43.52	-87.59
Prostate cancer				
PC-3	12.41	-35.46	2.31	-93.48
DU-145	38.96	-27.79	38.47	-93.96
Breast cancer				
MCF7	3.49	-76.15	-44.29	-73.81
MDA-MB-231/ATCC	23.15	-63.34	5.74	-76.74
HS 578T	-12.59	-39.90	-11.86	-40.25
BT-549	23.12	33.65	5.16	-73.63
T-47D	23.39	-62.31	16.08	-64.77
MDA-MB-468	-3.66	-62.73	-1.23	-83.99

20-40% growth inhibition; 40-50% growth inhibition; 50-70% growth inhibition; 70-80% growth inhibition; 80-90% growth inhibition; 90-100% growth inhibition; highly potent compounds.

Table 2. Compounds **6, 16, 17** and **20** with median growth inhibitory (GI_{50}, μM), total growth inhibitory (TGI, μM) and median lethal concentrations (LC_{50}, μM) of *in vitro* tumor cell lines at five different concentrations viz., 10^{-4}, 10^{-5}, 10^{-6}, 10^{-7} and 10^{-8} M

Compds.	Activity	I	II	III	IV	V	VI	VII	VIII	IX	MIG-MID[a]
6	GI_{50}	2.37	2.85	2.43	2.54	1.95	3.46	2.46	3.67	2.36	2.68
	TGI	6.50	9.66	5.52	23.2	4.18	22.6	11.8	9.13	6.72	11.0
	LC_{50}	[b]	9.54	30.2	46.6	11.8	26.9	8.29	[b]	92.7	32.3
16	GI_{50}	0.57	1.74	0.99	1.41	1.56	1.85	1.20	1.51	1.63	1.38
	TGI	2.17	3.67	2.55	3.04	3.18	3.88	2.72	3.07	4.08	3.15
	LC_{50}	16.3	14.2	6.53	5.98	6.52	6.84	6.27	6.25	8.74	8.63
17	GI_{50}	2.02	2.68	2.15	2.23	1.91	2.74	2.03	3.46	2.09	2.37
	TGI	6.11	6.65	4.73	11.8	4.04	11.5	7.36	6.66	5.55	7.16
	LC_{50}	[b]	7.76	7.90	8.47	7.43	[b]	7.83	[b]	[b]	7.88
20	GI_{50}	0.19	1.15	0.26	0.77	1.07	0.92	1.11	0.41	0.62	0.72
	TGI	0.58	2.59	0.69	1.92	2.48	2.30	2.25	1.49	1.86	1.80
	LC_{50}	[b]	5.58	2.75	[b]	5.79	5.20	5.60	4.33	[b]	4.88

I, leukemia; II, non-small cell lung cancer; III, colon cancer; IV, CNS cancer; V, melanoma; VI, ovarian cancer; VII, renal cancer; VIII, prostate cancer; IX, breast cancer. [a] Full panel mean-graph midpoint (μM). [b] Compounds showed values >100 μM.

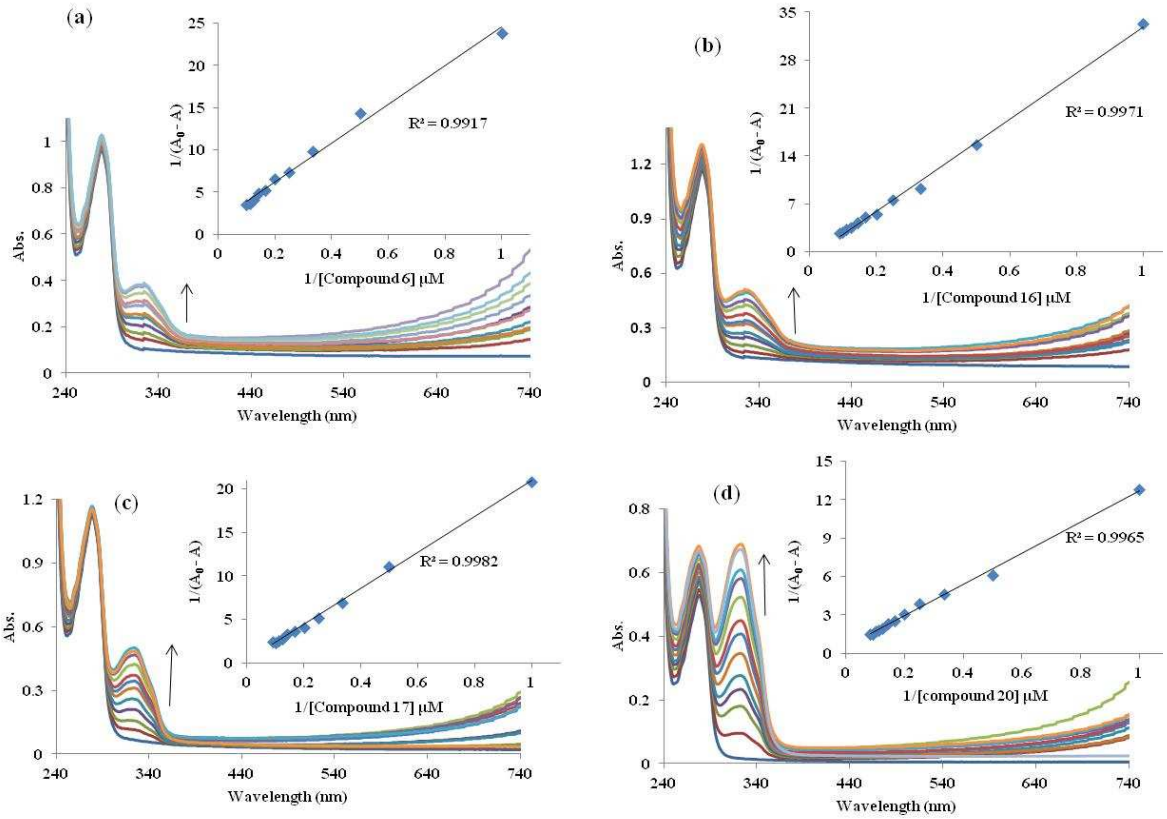

Figure 2. Absorption spectral changes of BSA (10 μM) in phosphate buffer upon addition of compounds **6** (a), **16** (b), **17** (c) and **20** (d) at 0-20 μM; Insets indicate Benesi–Hildebrand plot of 1/[A_0-A] vs. 1/[compounds] for binding of BSA with compounds **6** (a)**, 16** (b), **17** (c) and **20** (d) through absorption spectral titrations.

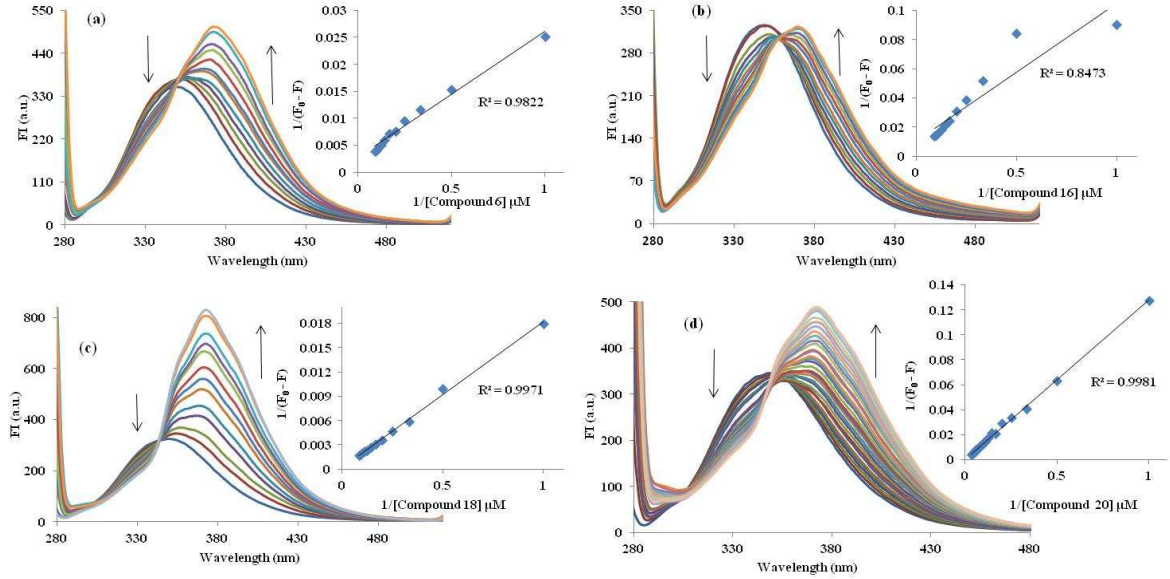

Figure 3. Fluorescence spectral changes of BSA (10 μM) in phosphate buffer upon addition of **6** (a), **16** (b), **17** (c) and **20** (d) at 0-20 μM. Insets indicate Benesi–Hildebrand plot of 1/[F_0-F] vs. 1/[compounds] for binding of BSA with compounds **6** (a), **16** (b), **17** (c) and **20** (d) through emission spectral titrations.

Table 3. Photophysical properties and binding constants of BSA with compounds **5-14**, **16**, **17** and **20**.

Sr. No.	Hyperchromicity (%) in absorption spectra	Enhancement (%) in emission spectra	Isoemissive point (nm)	Red shift in emission intensity (nm)	K (absorption spectra, M^{-1})	K (emission spectra, M^{-1})	n
5	72.93	63.43	350	24	7.0×10^4	6.9×10^4	1.24
6	72.31	49.74	350	25	9.7×10^4	5.7×10^4	0.91
7	65.29	68.99	341	22	1.0×10^5	5.4×10^4	1.67
8	75.98	77.53	339	22	8.5×10^4	2.6×10^4	1.19
9	85.95	57.22	345	23	8.4×10^4	5.7×10^4	0.90
10	68.72	73.21	343	25	1.2×10^5	5.4×10^4	1.61
11	70.53	69.01	347	22	6.3×10^4	1.3×10^5	0.94
12	90.60	71.82	340	23	9.5×10^4	8.0×10^4	1.01
13	88.44	42.06	352	24	1.2×10^4	1.8×10^5	1.14
14	85.87	23.12	349	17	1.0×10^5	1.6×10^5	1.58
16	72.27	22.78	357	20	1.2×10^5	3.2×10^4	1.47
17	86.80	71.83	341	23	1.0×10^5	7.9×10^4	0.99
20	97.67	49.10	349	22	1.0×10^5	4.2×10^7	0.87

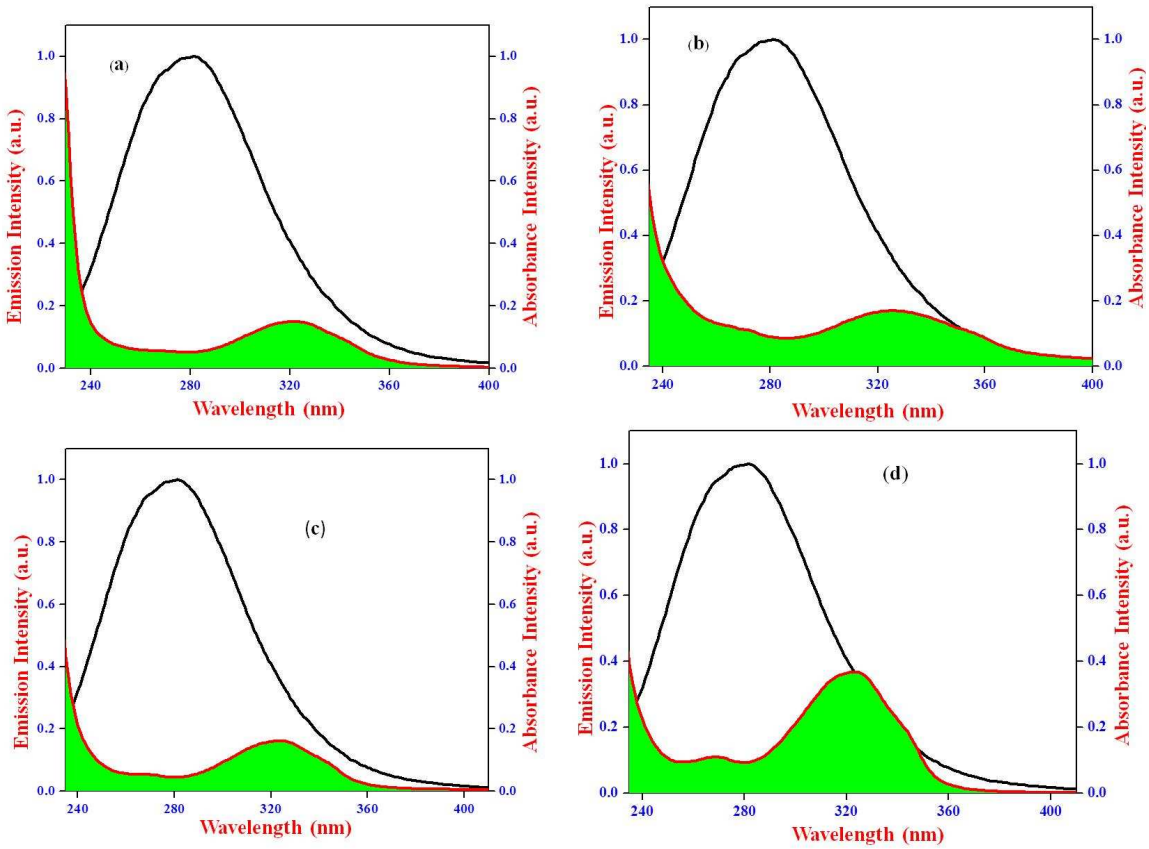

Figure 4. Overlap of the fluorescence emission spectra of BSA with UV-Visible absorption spectra of compounds **6** (a), **16** (b), **17** (c) and **20** (d).

Table 4. Forster energy transfer parameters for BSA and triazine-benzimidazoles (**5-14**, **16**, **17** and **20**).

Sr. No.	$\Phi_{(ligand)}$	$\Phi_{(complex)}$	% Overlapping area	Energy efficiency (E)	J (mol^{-1} cm^{-1} nm^4)	R_0 (nm)	r (nm)
5	0.31	0.20	24.98	37.50	1.25×10^{15}	4.41	4.78
6	0.24	0.29	30.29	2.63	1.28×10^{15}	4.43	7.90
7	0.23	0.23	9.60	26.86	1.35×10^{15}	4.47	5.28
8	0.30	0.25	2.30	21.62	1.21×10^{15}	4.40	5.45
9	0.36	0.24	14.50	24.41	1.29×10^{15}	4.44	5.38
10	0.34	0.22	19.35	29.30	1.28×10^{15}	4.43	5.14
11	0.23	0.27	19.46	15.58	1.24×10^{15}	4.41	5.81
12	0.32	0.22	10.78	31.71	1.46×10^{15}	4.53	5.13
13	0.38	0.29	26.74	7.39	1.42×10^{15}	4.51	6.94
14	0.28	0.28	18.57	11.28	1.44×10^{15}	4.52	6.40
16	0.22	0.29	27.55	9.56	1.59×10^{15}	4.59	6.61
17	0.31	0.20	23.80	3.74	1.39×10^{15}	4.49	7.62
20	0.30	0.31	37.63	3.10	1.63×10^{15}	4.61	7.98

Highlights

- A series of triazine-benzimidazole analogs has been synthesized.
- Compounds were evaluated *in vitro* for their antitumor activity.
- Four compounds showed excellent activity towards 60 human cancer cell lines.
- Interaction with bovine serum albumin has been determined.